14 (2022) 100085

Contents lists available at ScienceDirect

Journal of Non-Crystalline Solids: X

journal homepage: www.sciencedirect.com/journal/journal-of-non-crystalline-solids-x

Lines of invariant physics in the isotropic phase of the discotic Gay-Berne model

Saeed Mehri [a], Mohamed A. Kolmangadi [b], Jeppe C. Dyre [a,*], Trond S. Ingebrigtsen [a]

[a] "Glass and Time", IMFUFA, Dept. of Science and Environment, Roskilde University, P. O. Box 260, DK-4000 Roskilde, Denmark
[b] Bundesanstalt für Materialforschung und -Prüfung, Unter den Eichen 87, 12205 Berlin, Germany

A B S T R A C T

The Gay-Berne model is studied numerically with a choice of parameters allowing for the formation of a discotic liquid crystal at low temperatures. We show that the model has strong virial potential-energy correlations in the isotropic phase at high temperatures, i.e., it obeys the criterion for the existence of isomorphs, which are curves of approximately invariant structure and dynamics. These properties are demonstrated to be approximately invariant in reduced units along the isomorph studied. The isomorph is described well by the constant density-scaling exponent 11.5, a number that is significantly larger than the density-scaling exponents of various Lennard-Jones models that are always below 6.

1. Introduction

Liquid crystals constitute an intriguing family of materials with properties in-between the standard liquid and crystalline phases [1–3]. When the molecules are rod shaped, three main phases are typically found: isotropic, nematic, and smectic. The *isotropic* phase mimics the ordinary fluid phase with no long-range positional or orientational ordering. The *nematic* phase is characterized by long-range orientational order, but only short-range translational order. This phase is liquid in the sense of being able to flow freely, described by a viscosity that is not simply a scalar quantity. Optical properties of the nematic phase are likewise anisotropic, which is the basis for the use of this phase for applications in displays, etc. The *smectic* phase involves additional ordering by forming distinct layers, i.e., a partial positional order is introduced. There are different smectic phases, the most important ones being the *smectic A phase* in which the molecules are directionally ordered perpendicular to the layers and the *smectic C phase* involving molecules that are tilted relative to the layers. Both of these phases are positionally disordered in the layers. Other phases that may be encountered – depending on the molecule in question – are the *cholesteric* phase found only for chiral molecules and the so-called *blue* phase consisting of cubic structures of defects. As for any other first-order phase transition, it is possible to supercool the isotropic phase by cooling it fast below the transition temperatures of the partially ordered phases.

When the molecules instead of being rod-like are disc shaped, the system is termed a discotic liquid crystal [4–9]. Discotic liquid crystals can display various mesophases, the most common being the discotic columnar and nematic phases. The discotic nematic phase is similar to the standard nematic phase; here the short axes of the discs are aligned in one preferred direction. In the columnar phase the discs stack on top of each other into columns that organize into hexagonal or rectangular order. This phase is of interest for optoelectronic applications.

A standard model for numerical studies of rod-like liquid crystals is the Gay-Berne (GB) model [10–15]. This model has also been studied in other contexts than those relevant for liquid-crystal formation. Thus Angell and coworkers [16] in 2013 used the GB model to elucidate the possible existence of ideal glassformers, which are systems that vitrify upon cooling before becoming metastable with respect to crystal formation. This would imply that glasses may also form in the equilibrium liquid phase, contradicting the prevailing opinion that glasses always form from liquids that are supercooled with respect to the freezing transition. While the paper by Angell et al. [16] did not *prove* that this is possible, it presented a convincing case by reporting "that in the aspect range of maximum ellipsoid packing efficiency, various GB crystalline states that cannot be obtained directly from the liquid disorder spontaneously near 0 K and transform to liquids without any detectable enthalpy of fusion." This definitely suggests that the GB model (for certain aspect ratios) may be an ideal glassformer.

This paper presents a GB-model study which, like the 2013 paper by Angell et al., does not focus on liquid-crystal properties. We study the GB model for a set of parameters that allows for the formation of a discotic liquid-crystal phase at low temperatures. The focus is on the model's high-temperature isotropic phase with a view to investigate the possible

* Corresponding author.
E-mail address: dyre@ruc.dk (J.C. Dyre).

https://doi.org/10.1016/j.nocx.2022.100085
Received 11 November 2021; Received in revised form 19 February 2022; Accepted 21 February 2022
Available online 24 February 2022

existence of isomorphs. The motivation is the finding reported below that the high-temperature isotropic phase has strong virial potential-energy correlations, the condition for the existence of isomorphs, which are lines in the thermodynamic phase diagram of approximately invariant reduced-unit structure and dynamics [17–20].

2. Simulation methodology

2.1. The Gay-Berne potential

The GB potential was proposed as a simple model for rod-like molecules [10]. The potential takes the form of a Lennard-Jones interaction with characteristic length and energy scales that depend on the two molecules' orientations relative to one another. The pair potential is given by

$$v(\hat{\mathbf{r}}_{ij},\hat{\mathbf{e}}_i,\hat{\mathbf{e}}_j) = 4\varepsilon(\hat{\mathbf{r}}_{ij},\hat{\mathbf{e}}_i,\hat{\mathbf{e}}_j)\left[\left(\frac{\sigma_s}{\rho_{ij}}\right)^{12} - \left(\frac{\sigma_s}{\rho_{ij}}\right)^{6}\right], \tag{1a}$$

$$\rho_{ij} = r_{ij} - \sigma(\hat{\mathbf{r}}_{ij},\hat{\mathbf{e}}_i,\hat{\mathbf{e}}_j) + \sigma_s. \tag{1b}$$

Here r_{ij} is the distance between the centers of the molecules i and j, $\hat{\mathbf{r}}_{ij}$ is the unit vector along $\mathbf{r}_{ij} = \mathbf{r}_i - \mathbf{r}_j$, and $\hat{\mathbf{e}}_i$ and $\hat{\mathbf{e}}_j$ are unit vectors along the major axes of each molecule. The GB model is characterized by

$$\sigma(\hat{\mathbf{r}}_{ij},\hat{\mathbf{e}}_i,\hat{\mathbf{e}}_j) = \sigma_s\left[1 - \frac{\chi}{2}\left(\frac{(\hat{\mathbf{e}}_i\cdot\hat{\mathbf{r}}_{ij} + \hat{\mathbf{e}}_j\cdot\hat{\mathbf{r}}_{ij})^2}{1+\chi(\hat{\mathbf{e}}_i\cdot\hat{\mathbf{e}}_j)} + \frac{(\hat{\mathbf{e}}_i\cdot\hat{\mathbf{r}}_{ij} - \hat{\mathbf{e}}_j\cdot\hat{\mathbf{r}}_{ij})^2}{1-\chi(\hat{\mathbf{e}}_i\cdot\hat{\mathbf{e}}_j)}\right)\right]^{-1/2}, \tag{2a}$$

with

$$\chi = \frac{\kappa^2-1}{\kappa^2+1} \quad \text{and} \quad \kappa = \sigma_e \Big/ \sigma_s. \tag{2b}$$

Here χ is a shape-anisotropy parameter and κ quantifies the elongation of the molecule. The case κ=1, χ=0 corresponds to spherical particles, $\kappa \to \infty$, $\chi \to 1$ corresponds to very long rods, and $\kappa \to 0$, $\chi \to -1$ corresponds to very thin disks.

The energy term appearing in the GB potential is given by

$$\epsilon(\hat{\mathbf{r}}_{ij},\hat{\mathbf{e}}_i,\hat{\mathbf{e}}_j) = \epsilon_0\epsilon_1^{\nu}(\hat{\mathbf{e}}_i,\hat{\mathbf{e}}_j)\epsilon_2^{\mu}(\hat{\mathbf{r}}_{ij},\hat{\mathbf{e}}_i,\hat{\mathbf{e}}_j), \tag{3a}$$

in which

$$\epsilon_1(\hat{\mathbf{e}}_i,\hat{\mathbf{e}}_j) = \left(1-\chi^2(\hat{\mathbf{e}}_i\cdot\hat{\mathbf{e}}_j)^2\right)^{-1/2} \tag{3b}$$

$$\epsilon_2(\hat{\mathbf{r}}_{ij},\hat{\mathbf{e}}_i,\hat{\mathbf{e}}_j) = 1 - \frac{\chi'}{2}\left(\frac{(\hat{\mathbf{e}}_i\cdot\hat{\mathbf{r}}_{ij} + \hat{\mathbf{e}}_i\cdot\hat{\mathbf{r}}_{ij})^2}{1+\chi'(\hat{\mathbf{e}}_i\cdot\hat{\mathbf{e}}_j)} + \frac{(\hat{\mathbf{e}}_i\cdot\hat{\mathbf{r}}_{ij} - \hat{\mathbf{e}}_j\hat{\mathbf{r}}_{ij})^2}{1-\chi'(\hat{\mathbf{e}}_i\cdot\hat{\mathbf{e}}_j)}\right). \tag{3c}$$

Here the "energy anisotropy parameter" χ' is defined by

$$\chi' = \frac{\kappa'^{1/\mu}-1}{\kappa'^{1/\mu}+1}, \quad \text{with} \quad \kappa' = \epsilon_{ss} \Big/ \epsilon_{ee} \tag{3d}$$

The parameters ϵ_{ss} and ϵ_{ee} are the well depth of the potential in the side-to-side and end-to-end configurations, respectively, while ν and μ are exponents. In the original GB paper, rod-like molecules were simulated with parameters in the notation GB(κ, κ', μ, ν) = GB(3,5,2,1).

2.2. The discotic GB model

To mimic a discotic liquid-crystal using the GB potential one replaces σ_s by σ_e:

$$v(\hat{\mathbf{r}}_{ij},\hat{\mathbf{e}}_i,\hat{\mathbf{e}}_j) = 4\epsilon(\hat{\mathbf{r}}_{ij},\hat{\mathbf{e}}_i,\hat{\mathbf{e}}_j)\left[\left(\frac{\sigma_e}{\rho_{ij}}\right)^{12} - \left(\frac{\sigma_e}{\rho_{ij}}\right)^{6}\right] \tag{4a}$$

$$\rho_{ij} = r_{ij} - \sigma(\hat{\mathbf{r}}_{ij},\hat{\mathbf{e}}_i,\hat{\mathbf{e}}_j) + \sigma_e, \tag{4b}$$

keeping everything else the same. This choice avoids the unphysical effects [21] previously described by Bates and Luckhurst [12] and used by Cienega-Cacerez et al. [22] to obtain a discogen phase diagram for GB (0.345,0.2,1,2). The parameter σ_e defines the thickness of the discogen.

2.3. Simulation details

The system studied consists of $N = 2048$ disks. The potential is truncated, but not shifted, at r_c=1.6σ_s following the above-mentioned paper. Units are defined by putting $\sigma_s = 1$ and $\varepsilon_0 = 1$. We use the standard Nosé-Hoover *NVT* algorithm for the center-of-mass motion [23] and the IMP algorithm of Fincham for the rotational motion [24] with 10 iterations per step. We find that the latter algorithm, although not rigorously time reversible, conserves the energy very well. *NVT* simulations for the rotational motion follow the "Toxvaerd" version of the Finchham algorithm [25] (not the Berendsen version outlined in Ref. [24]). Two independent thermostats were applied for translation and rotational motion (using a single thermostat did not give noticeable differences). The moment of inertia of the discs was $I = 1$. Equilibration and production runs consisted of 5×10^6 time steps each with Δt=0.0005. The GB implementation was compared to the literature comprising also, e.g., quaternion algorithms for the standard GB model; full agreement was established for time-correlation functions, etc.

2.4. Isomorphs

We study in this paper an isomorph in the high-temperature isotropic phase. Isomorphs are defined as curves of constant excess entropy S_{ex}. They can be generated numerically by utilizing the following general statistical-mechanical identity in which ρ is the particle density and T is the temperature [18].

$$\gamma \equiv \left(\frac{\partial lnT}{\partial ln\rho}\right)_{S_{ex}} = \frac{\langle \Delta U \Delta W\rangle}{\langle (\Delta U)^2\rangle} \tag{5}$$

Here U is the potential energy and W is the virial. This equation is used as follows. At a given state point (ρ, T) one calculates the fluctuation average on the right hand side from an *NVT* simulation. If, for instance, this results in γ=3, Eq. (5) implies that if density is increased by 1%, temperature should be increased by 3% to keep the excess entropy constant. In this way one can step-by-step trace out an isomorph in the thermodynamic phase diagram. We used the fourth-order Runge-Kutta algorithm to do this numerically, which is more accurate than the simple Euler algorithm [26]. We increased the density by 1% at each step and covered an overall density variation of 20%.

The dynamical behavior along the isomorph is analyzed in terms of time-autocorrelation functions defined by

$$\phi_A(t) = \frac{\langle \mathbf{A}(t_0)\cdot\mathbf{A}(t_0+t)\rangle}{\langle \mathbf{A}(t_0)\cdot\mathbf{A}(t_0)\rangle} \tag{6}$$

where $\mathbf{A}(t)$ is a vector dynamical property referring to a given molecule at time t. We evaluate below $\phi_A(t)$ for $\mathbf{A}$ being the velocity of the molecule's center-of-mass, as well as the angular velocity. To study the orientational motion we calculate the self-particle orientational correlation functions,

$$\phi_l(t) = \langle P_l(\hat{\mathbf{e}}_i(t_0)\cdot\hat{\mathbf{e}}_i(t_0+t))\rangle \tag{7}$$

where P_l is a Legendre polynomial (l=1 and 2) and i is a particle index. In the above expressions, the angular brackets imply an average over particles and time origins. The spatial orientational correlation function is defined as follows

$$G_2(r) \equiv \langle P_2(\hat{\mathbf{e}}_i\cdot\hat{\mathbf{e}}_j)\rangle \tag{8}$$

in which the average involves the pairs of particles i and j that are the distance r apart.

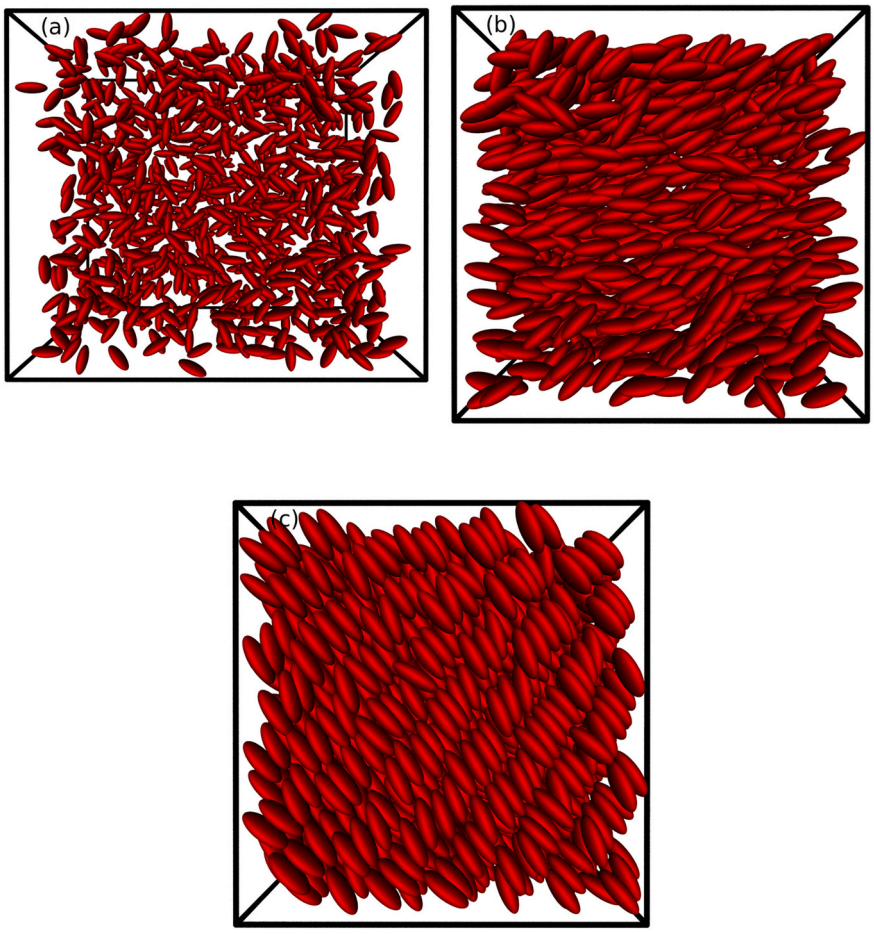

Fig. 1. Snapshots of the discotic GB model in thermal equilibrium at three state points (schematic drawings). (a) shows the isotropic liquid phase at (ρ, T) = (0.6,2.6); (b) shows the nematic phase at (ρ, T) = (2.3,2.6); (c) shows the columnar phase at (ρ, T) = (3.0,2.6).

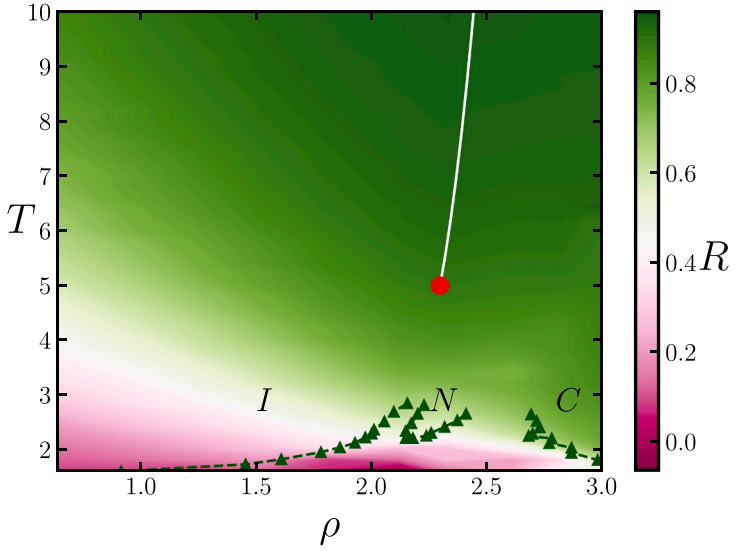

Fig. 2. The phase diagram of the discotic GB(0.345,0.2,1,2) model with R values (Eq. (9)) given by the color code to the right. The triangular symbols delimit the phase boundaries [22]. I stands for the isotropic, N for the nematic, and C for the columnar phase. The red filled circle is the isomorph reference state point (ρ, T) = (2.3,5.0), the white curve is the isomorph (which is studied up to T=43).

Table 1
The density ρ, temperature T, correlation coefficient R (Eq. (9)), and density-scaling exponent γ (Eq. (5)) of the state points studied along the isomorph. At each step density was increased by 1%. For the ρ=2.3 isochore we used same temperatures as in the table.

ρ	T	R	γ
2.300	5.000	0.8919	10.72
2.323	5.569	0.9087	10.99
2.346	6.222	0.9236	11.25
2.370	6.964	0.9354	11.41
2.393	7.805	0.9449	11.53
2.417	8.753	0.9511	11.56
2.441	9.821	0.9567	11.58
2.466	11.02	0.9598	11.57
2.491	12.36	0.9626	11.56
2.515	13.87	0.9646	11.53
2.541	15.55	0.9657	11.48
2.566	17.43	0.9672	11.46
2.592	19.53	0.9676	11.43
2.618	21.88	0.9678	11.41
2.644	24.50	0.9677	11.37
2.670	27.43	0.9673	11.33
2.697	30.71	0.9673	11.32
2.724	34.36	0.9673	11.30
2.751	38.45	0.9668	11.28
2.779	43.01	0.9662	11.26

2.5. Units

As mentioned, quantities are reported using the length unit σ_s and the energy unit ε_0 (MD units). We apply, however, also the "macroscopic" unit system based on the length unit $\rho^{-1/3}$ and the energy unit k_BT. Note that these so-called reduced units vary with state point. Isomorph invariance of structure and dynamics applies only when the quantities in question are given in reduced units [18], which is marked below by a tilde.

3. Phase diagram of the discotic GB model

Fig. 1 shows snapshots from simulations of the discotic GB model in the isotropic, nematic, and columnar phases, respectively. The pictures represent typical thermal equilibrium configurations. Each simulation was started from a perfect crystal at unit density after which density and temperature were changed to gradually reach the required values. To ensure that the system at the density and temperature aimed for is in equilibrium, similar simulations were performed starting from a high density and temperature and gradually decreasing those to the desired values.

The thermodynamic phase diagram of the model is investigated in Fig. 2 reporting the virial potential-energy correlation coefficient R defined [17] by

$$R = \frac{\langle \Delta U \Delta W \rangle}{\sqrt{\langle (\Delta U)^2 \rangle \langle (\Delta W)^2 \rangle}} \tag{9}$$

Here Δ denotes the deviation from the thermal average and the sharp brackets denote equilibrium canonical constant-volume (NVT) averages. The condition defining "strong UW correlations" is R>0.9. This is the pragmatic criterion used for identifying regions of the phase diagram in which a given system is expected to have isomorphs, implying approximately invariant reduced-unit structure and dynamics [18].

In the figure, the letters "I", "N", and "C" denote the isotropic, nematic, and columnar phases, delimited by the triangular symbols (data taken from Ref. 22). The color coding reflects the value of R. We see that for temperatures above 5 and densities above about 2.4, i.e., well into the high-temperature isotropic phase, R is large enough to qualify for strong virial potential-energy correlation. The isomorph studied in this paper (white line) was generated as described in Sec. 2.3 starting from the reference state point (ρ, T) = (2.3,5.0). We proceed to investigate how different probes of structure and dynamics vary along this isomorph.

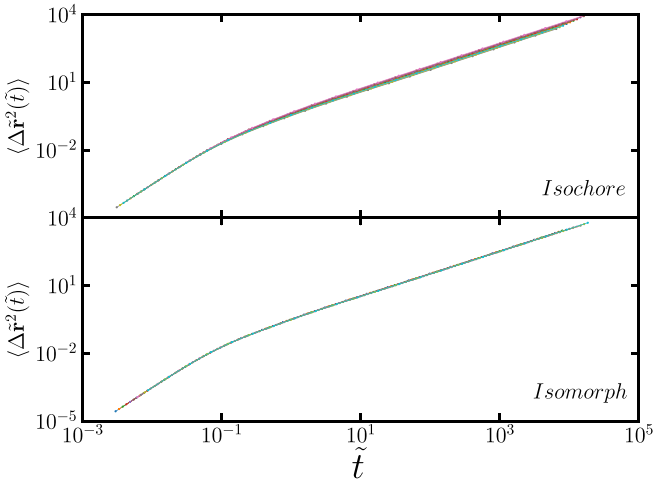

Fig. 3. Comparing the reduced-unit MSD along the isochore and the isomorph. At short times both figures exhibit a ballistic regime where the MSD is proportional to t^2; by the definition of reduced units the ballistic regime is the same at all state points. At long times both figures exhibit a diffusive regime where the MSD is proportional to t. Only along the isomorph do the data collapse in both regimes. Data are shown for 20 state points with 2.30<ρ<2.78 and 5<T<43.

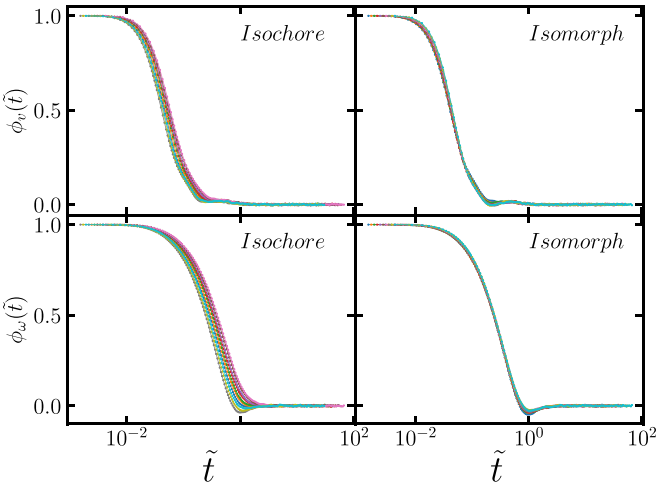

Fig. 4. Upper panel: center-of-mass velocity autocorrelation function as a function of the reduced time. Lower panel: angular velocity autocorrelation function.

4. Comparing the isomorph to the ρ=2.3 isochore

The discotic GB model has more structural and dynamic signatures than a simple liquid for which there is basically just the radial distribution function (RDF) $g(r)$ and the time-dependent mean-square displacement (MSD). This section investigates to which degree structure and dynamics are invariant along the isomorph (white line in Fig. 2). Quantities are reported in reduced units (Sec. II.E). In order to put the isomorph findings into perspective, we compare to the variation of the same quantities along the ρ=2.3 isochore over the same temperature range as along the isomorph (5<T<43). Table 1 gives data for the isomorph state points studied.

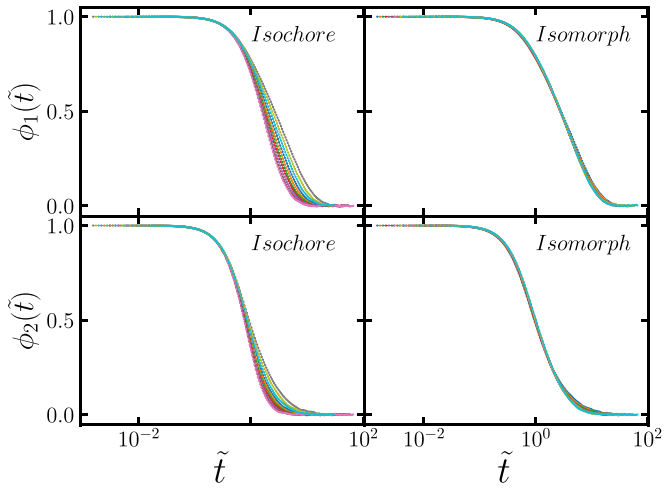

Fig. 5. First order (upper panel) and second order (lower panel) orientational autocorrelation functions (Eq. (7)).

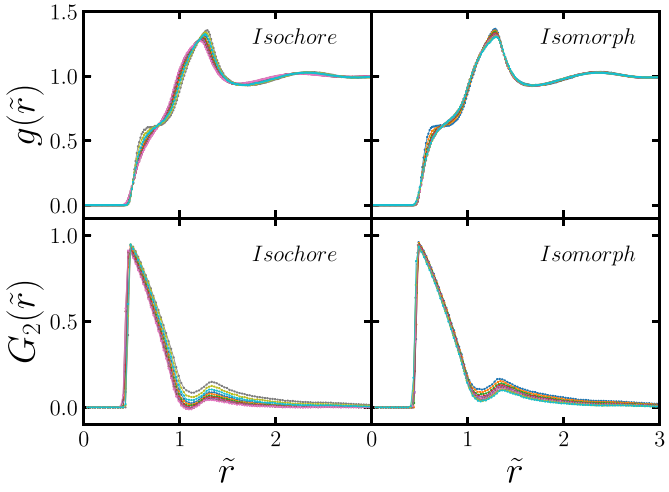

Fig. 6. Radial distribution function and orientational correlation function plotted as functions of the reduced distance along the isochore and the isomorph.

4.1. Dynamics

Fig. 3 compares the reduced-unit MSD along the isochore and the isomorph. Only along the isomorph is there invariance. Such data are typical for systems with isomorphs, so-called R-simple systems, and the data confirm the prediction of invariant dynamics along an isomorph [18]. One can think of an isomorph as a line in the phase diagram along which all physics relating to the positions and motion of the particles relative to one another is the same. Thus if one imagines filming the molecules at two different state points on a given isomorph, the same movie is recorded except for a scaling of space and time. This is the prediction for perfect isomorphs which, however, only exist in systems for which the potential-energy function is homogenous (implying R=1). For more realistic systems, isomorph invariance is approximate.

Fig. 4 gives data for two different velocity autocorrelation functions. The upper row shows the reduced center-of-mass velocity autocorrelation function along the isochore (left) and along the isomorph (right). We see data collapse along the latter, but not along the former. This is not surprising in view of Fig. 3 because the velocity autocorrelation function is two times the second derivative of the MSD. The two lower figures report the angular velocity autocorrelation functions, a quantity that has no analog in the standard Lennard-Jones model. Again we

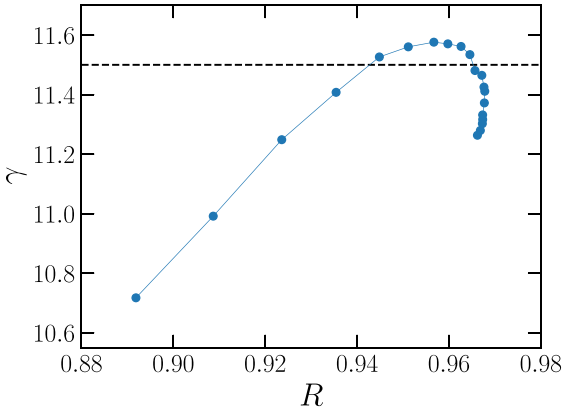

Fig. 7. Plot of γ versus R along the isomorph. The lower left corner is the reference state point (ρ, T) = (2.3,5.0); moving to higher temperatures and densities corresponds to moving to the upper right.

observe dynamic invariance along the isomorph, but not along the isochore.

Fig. 5 shows data for the first- and second-order orientational time-autocorrelation functions. In all cases, the function is unity at short times and decays to zero at long times. Only along the isomorph is the decay invariant to a good approximation.

We conclude that the reduced-unit dynamic characteristics are approximately invariant along the isomorph, but not along an isochore with the same temperature variation. This confirms the isomorph-theory prediction.

4.2. Structure

Next we report data for the reduced-unit structure. The upper panel of Fig. 6 shows the ordinary center-of-mass RDF along the isochore and the isomorph. The data are more invariant along the latter, but this time the difference is less striking. A similar observation is made for the spatial orientational correlation function (Eq. (8)) plotted in the lower figures.

Isomorph invariance of the isotropic phase of the discotic GB model is more pronounced for the dynamics than for the structure. A similar observation has been made in some liquids for which the height of the first peak of the radial distribution function may vary along an isomorph if the density-scaling exponent varies significantly [27]. This is consistent with the recent finding that the so-called bridge function is isomorph invariant [28], because an invariant bridge function implies that the RDF cannot be rigorously invariant.

5. Applying the constant-exponent density-scaling framework

Turning back to the dynamics, we now seek to interpret it in terms of density-scaling in its classical version for which the density-scaling exponent γ is assumed to be a material constant, i.e., not to vary with state point [29,30]. In this version, dynamic quantities are predicted to be a unique function of ρ^{γ}/T when plotted in reduced units.

In isomorph theory γ is the generally state-point-dependent quantity defined in Eq. (5). Fig. 7 shows how this γ and the virial potential-energy correlation coefficient R vary along the isomorph. The correlation coefficient increases as temperature and density are increased moving toward the upper right corner. At the same time, γ increases and goes through a maximum.

We calculated the average value of the isomorph-theory density-scaling exponent (Eq. (5)) along the four isochores given by ρ=2.2, ρ=2.3, ρ=2.4, and ρ=2.5 with temperatures obeying $T \in$ [5,43],[4,32], [10,32], and [11,43], respectively. The results is

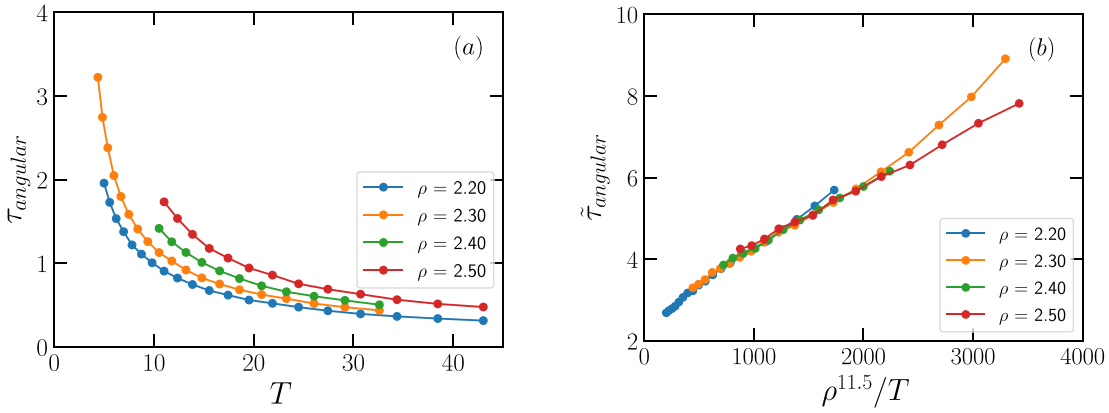

Fig. 8. (a) Average angular relaxation time as a function of temperature along four isochores with density varying from ρ=2.2 to ρ=2.5. (b) The same data for the average angular relaxation time plotted in reduced units as a function of the constant-exponent density-scaling variable ρ^{γ}/T with γ=11.5.

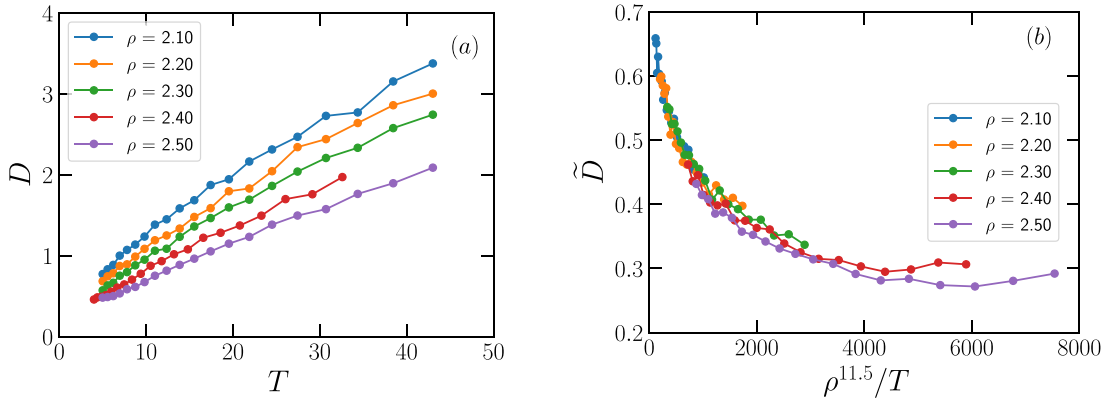

Fig. 9. (a) Diffusion coefficient as a function of temperature along five isochores with density varying from ρ=2.1 to ρ=2.5. (b) The same data plotted in reduced units as a function of the density-scaling variable ρ^{γ}/T with γ=11.5.

$$\gamma = 11.5. \tag{10}$$

This number is much larger than the density-scaling exponents found in standard Lennard-Jones models, which are never above 6 [17,18,31]. This emphasizes how different the GB model is from point-particle Lennard-Jones models, which also have isomorphs [32]. We conclude that the existence of isomorphs of the GB model is not inherited in a trivial way from the standard Lennard-Jones model.

Fig. 8(a) shows the average relaxation time of the angular autocorrelation function identified as the time at which this has reached the value 0.2, plotted as a function of the temperature along four isochores. Fig. 8(b) tests the constant-exponent version of density scaling with the average γ of Eq. (10). We find a good collapse for most data, with deviations at the longest relaxation times (lowest temperatures). This is where the density-scaling exponent deviates most from its average value 11.5, compare Fig. 7, i.e., where the constant-exponent approximation is expected to work less well.

Fig. 9 shows a similar figure for the center-of-mass diffusion coefficient D (with the additional isochore $\rho = 2.1$), extracted from the long-time behavior of the MSD. Fig. 9(a) shows the data for D as a function of the temperature and (b) shows the reduced-unit diffusion coefficient as a function of $\rho^{11.5}/T$. We again see a good data collapse.

6. Discussion

This paper has demonstrated the applicability of isomorph theory to the high-temperature isotropic phase of the discotic Gay-Berne model. We have traced out an isomorph and shown that along it the reduced-unit dynamics is invariant to a good approximation, while it is not invariant along an isochore with the same temperature variation. Dynamic invariance applies not only for the standard mean-square displacement and velocity autocorrelation functions as a function of the reduced time (note that these are not independent quantities), invariance applies also for the first- and second-order orientational time-autocorrelation functions. The reduced-unit structure quantified by the radial distribution function and the corresponding spatial orientational correlation function are also isomorph invariant to a good approximation, although these quantities vary relatively little even along the isochore.

The isomorph-theory density-scaling exponent γ varies between 10.7 and 11.6, with the majority of exponents found close to 11.6 when studied along, e.g., the ρ=2.5 isochore. The density-scaling exponent averaged over the four isochores is 11.5. It is not clear why this value is so much larger than density-scaling exponents of the standard and various binary Lennard-Jones models. Constant-exponent density scaling applies with this value of γ, i.e., a good collapse is observed when the reduced-unit angular relaxation time and the reduced-unit diffusion coefficient are plotted as functions of $\rho^{11.5}/T$.

This paper presented the first application of isomorph theory to a liquid-crystal model. Future works will focus on other GB models and on the possibility of extending isomorph theory to ordered phases such as the nematic phase. In Ref. 14 density scaling was shown to apply for the GB model in the nematic phase with parameters corresponding to rod-like particles. For the current GB discotic liquid-crystal model we needed to go to high temperatures to find strong virial potential-energy correlations, but the fact that density scaling applies for the ordered

phases of the GB model for other parameters than those studied here suggests that isomorphs may also exist in the model's ordered phases. This is the subject of an ongoing investigation.

7. Conclusion

We have demonstrated the existence of isomorphs in the isotropic phase of the Gay-Berne liquid-crystal model. This shows that the model has the hidden-scale-invariance symmetry [33] that basically removes one dimension from the two-dimensional thermodynamic phase diagram. In other systems like supercooled molecular liquids, the existence of isomorphs implies specific predictions of how the system behaves under high pressure [34]; we expect that similar predictions can be made for high-pressure experiments on liquid crystals.

Declaration of Competing Interest

None.

Acknowledgments

This paper is dedicated to the memory of Austen Angell, a wonderful person and an eminent scientist who was always curious and supportive in relation to other people's works. The work was supported by the VILLUM Foundation's *Matter* Grant (No. 16515).

References

[1] G.R. Luckhurst, G.W. Gray (Eds.), The Molecular Physics of Liquid Crystals, Academic Press, New York, 1979.
[2] M.P. Allen, Molecular simulation of liquid crystals, Mol. Phys. 117 (2019) 2391.
[3] Wikipedia article "Liquid Crystal", (2021).
[4] S. Kumar, Discotic liquid crystal-nanoparticle hybrid systems, NPG Asia Mater. 6 (2014), e82.
[5] S. Laschat, A. Baro, N. Steinke, F. Giesselmann, C. Haegele, G. Scalia, R. Judele, E. Kapatsina, S. Sauer, A. Schreivogel, M. Tosoni, Discotic liquid crystals: from tailor-made synthesis to plastic electronics, Angew. Chem. Int. Ed. 46 (2007) 4832.
[6] T. Wöhrle, I. Wurzbach, J. Kirres, A. Kostidou, N. Kapernaum, J. Litterscheidt, J. C. Haenle, P. Staffeld, A. Baro, F. Giesselmann, S. Laschat, Discotic liquid crystals, Chem. Rev. 116 (2016) 1139.
[7] R.J. Bushby, K. Kawata, Liquid crystals that affected the world: discotic liquid crystals, Liq. Cryst. 38 (2011) 1415.
[8] M.A. Kolmangadi, A. Yildirim, K. Sentker, M. Butschies, A. Bühlmeyer, P. Huber, S. Laschat, A. Schönhals, Molecular dynamics and electrical conductivity of guanidinium based ionic liquid crystals: influence of cation headgroup configuration, J. Mol. Liq. 330 (2021), 115666.
[9] A. Yildirim, M.A. Kolmangadi, A. Buühlmeyer, P. Huber, S. Laschat, A. Schönhals, Electrical conductivity and multiple glassy dynamics of crown ether-based columnar liquid crystals, J. Phys. Chem. B 124 (2020) 8728.
[10] J.G. Gay, B.J. Berne, Modification of the overlap potential to mimic a linear site–site potential, J. Chem. Phys. 74 (1981) 3316.
[11] E. De Miguel, L.F. Rull, M.K. Chalam, K.E. Gubbins, Liquid crystal phase diagram of the Gay-Berne fluid, Mol. Phys. 74 (1991) 405.
[12] M.A. Bates, G.R. Luckhurst, Computer simulation studies of anisotropic systems. XXVI. Monte Carlo investigations of a Gay–Berne discotic at constant pressure, J. Chem. Phys. 104 (1996) 6696.
[13] S. Ravichandran, A. Perera, M. Moreau, B. Bagchi, Universality in the fast orientational relaxation near isotropic–nematic transition, J. Chem. Phys. 109 (1998) 7349.
[14] K. Satoh, Thermodynamic scaling of dynamic properties of liquid crystals: verifying the scaling parameters using a molecular model, J. Chem. Phys. 139 (2013), 084901.
[15] A. Humpert, M.P. Allen, Elastic constants and dynamics in nematic liquid crystals, Mol. Phys. 113 (2015) 2680.
[16] V. Kapko, Z. Zhao, D.V. Matyushov, C.A. Angell, Ideal glassformers vs ideal glasses: studies of crystal-free routes to the glassy state by "potential tuning" molecular dynamics, and laboratory calorimetry, J. Chem. Phys. 138 (2013) 12A549.
[17] N.P. Bailey, U.R. Pedersen, N. Gnan, T.B. Schrøder, J.C. Dyre, Pressure-energy correlations in liquids. I. Results from computer simulations, J. Chem. Phys. 129 (2008), 184507.
[18] N. Gnan, T.B. Schrøder, U.R. Pedersen, N.P. Bailey, J.C. Dyre, Pressure-energy correlations in liquids. IV. "Isomorphs" in liquid phase diagrams, J. Chem. Phys. 131 (2009), 234504.
[19] T.S. Ingebrigtsen, T.B. Schrøder, J.C. Dyre, What is a simple liquid? Phys. Rev. X 2 (2012), 011011.
[20] T.B. Schrøder, J.C. Dyre, Simplicity of condensed matter at its core: generic definition of a Roskilde-simple system, J. Chem. Phys. 141 (2014), 204502.
[21] A.P.J. Emerson, G.R. Luckhurst, S.G. Whatling, Computer simulation studies of anisotropic systems. XXIII. The Gay-Berne discogen, Mol. Phys. 82 (1994) 113.
[22] O. Cienega-Cacerez, J.A. Moreno-Razo, E. Diaz-Herrera, E.J. Sambriski, Phase equilibria, fluid structure, and diffusivity of a discotic liquid crystal, Soft Matter 10 (2014) 3171.
[23] W.G. Hoover, Canonical dynamics: equilibrium phase-space distributions, Phys. Rev. A 31 (1985) 1695.
[24] D. Fincham, Leapfrog rotational algorithms for linear molecules, Mol. Simul. 11 (1993) 79.
[25] D. Fincham, Leapfrog rotational algorithms, Mol. Simul. 8 (1992) 165.
[26] E. Attia, J.C. Dyre, U.R. Pedersen, Extreme case of density scaling: the Weeks-Chandler-Andersen system at low temperatures, Phys. Rev. E 103 (2021), 062140.
[27] A.K. Bacher, T.B. Schrøder, J.C. Dyre, The EXP pair-potential system. II. Fluid phase isomorphs, J. Chem. Phys. 149 (2018), 114502.
[28] F.L. Castello, P. Tolias, J.C. Dyre, Testing the isomorph invariance of the bridge functions of Yukawa one-component plasmas, J. Chem. Phys. 154 (2021), 034501.
[29] A. Tölle, Neutron scattering studies of the model glass former ortho-terphenyl, Rep. Prog. Phys. 64 (2001) 1473.
[30] C. Alba-Simionesco, A. Cailliaux, A. Alegría, G. Tarjus, Scaling out the density dependence of the α relaxation in glass-forming polymers, Europhys. Lett. 68 (2004) 58.
[31] N.P. Bailey, U.R. Pedersen, N. Gnan, T.B. Schrøder, J.C. Dyre, Pressure-energy correlations in liquids. II. Analysis and consequences, J. Chem. Phys. 129 (2008), 184508.
[32] T.B. Schrøder, N. Gnan, U.R. Pedersen, N.P. Bailey, J.C. Dyre, Pressure-energy correlations in liquids. V. Isomorphs in generalized lennard-jones systems, J. Chem. Phys. 134 (2011), 164505.
[33] J.C. Dyre, Hidden scale invariance in condensed matter, J. Phys. Chem. B 118 (2014) 10007.
[34] H.W. Hansen, A. Sanz, K. Adrjanowicz, B. Frick, K. Niss, Evidence of a one-dimensional thermodynamic phase diagram for simple glass-formers, Nat. Commun. 9 (2018) 518.